Journal of Dermatological Science 78 (2015) 197–205

Contents lists available at ScienceDirect

Journal of Dermatological Science

journal homepage: www.jdsjournal.com

Analysis of unique mutations in the *LPAR6* gene identified in a Japanese family with autosomal recessive woolly hair/hypotrichosis: Establishment of a useful assay system for LPA_6

Ryota Hayashi [a,b], Asuka Inoue [c,d], Yasushi Suga [e], Junken Aoki [c,f], Yutaka Shimomura [a,b,*]

[a] Laboratory of Genetic Skin Diseases, Niigata University Graduate School of Medical and Dental Sciences, Niigata, Japan
[b] Division of Dermatology, Niigata University Graduate School of Medical and Dental Sciences, Niigata, Japan
[c] Laboratory of Molecular and Cellular Biochemistry, Graduate School of Pharmaceutical Sciences, Tohoku University, Sendai, Japan
[d] PRESTO, Japan Science and Technology Agency (JST), Kawaguchi, Japan
[e] Department of Dermatology, Juntendo University Urayasu Hospital, Urayasu, Japan
[f] CREST, JST, Kawaguchi, Japan

ARTICLE INFO

Article history:
Received 11 December 2014
Received in revised form 14 February 2015
Accepted 4 March 2015

Keywords:
Woolly hair
Hypotrichosis
LPAR6
LPA_6
LIPH

ABSTRACT

Background: Woolly hair (WH) is a hair shaft anomaly characterized by tightly-curled hair and is frequently associated with hypotrichosis. Non-syndromic forms of WH can show either autosomal dominant or recessive inheritance. The autosomal recessive form of WH (ARWH) is caused by mutations in either lipase H (*LIPH*) or lysophosphatidic acid receptor 6 (*LPAR6*) gene, encoding an LPA-producing enzyme PA-$PLA_1\alpha$ and an LPA receptor LPA_6, respectively.
Objective: To define the molecular basis of ARWH/hypotrichosis in a Japanese family.
Methods: We performed mutational analysis of candidate genes and a series of expression and in vitro functional analyses, which we improved in this study, to determine the consequences resulting from the mutations identified in the family.
Results: Novel compound heterozygous *LPAR6* mutations were identified in the patient. One was a nonsense mutation c.756T > A (p.Tyr252*); the other was a large insertion mutation within the promoter region of *LPAR6*. Expression studies detected *LPAR6* mRNA only from the c.756T > A allele in the patient's hair follicles, suggesting that the insertion in the other allele disrupted the *LPAR6* promoter and thus led to a failure of transcription. Furthermore, an improved LPA_6 functional assay developed in this study demonstrated aberrant expression and a subsequent loss of function of the p.Tyr252*-mutant protein.
Conclusion: Through establishing a useful assay system for LPA_6, our results further underscore the crucial roles of *LPAR6* in hair follicle development and hair growth in humans at molecular levels.

1. Introduction

Woolly hair (WH) is a hair shaft anomaly that is characterized by short, thin, and tightly curled hair. Scalp hairs of affected individuals with WH typically stop growing at a few inches. In addition, hair loss can progress gradually with aging and result in hypotrichosis. Therefore, WH is considered to be a kind of hair growth deficiency [1]. WH is generally classified into syndromic and non-syndromic forms. In the syndromic forms of WH, affected individuals show not only hair symptoms, but also various cutaneous and non-cutaneous complications, such as palmoplantar keratoderma, bone anomaly, and heart failure [2]. By contrast, WH is the only main symptom in the non-syndromic forms, although other cutaneous findings (such as dry skin and keratosis pilaris) can appear in some cases [3]. The non-syndromic forms of WH show either an autosomal dominant (ADWH; OMIM 194300) or autosomal recessive (ARWH; OMIM 278150/604379) inheritance [1]. ADWH results

Abbreviations: WH, woolly hair; AD, autosomal dominant; AR, autosomal recessive; IRS, inner root sheath; HF, hair follicle; LPA, lysophosphatidic acid; GPCR, G protein–coupled receptor; PCR, polymerase chain reaction; RT, reverse transcription; AP, alkaline phosphatase; WT, wild-type; *p*-NPP, *p*-nitrophenylphosphate.

* Corresponding author at: Laboratory of Genetic Skin Diseases, Niigata University Graduate School of Medical and Dental Sciences, 1-757 Asahimachi-dori, Chuo-ku, Niigata 951-8510, Japan. Tel.: +81 25 227 2025; fax: +81 25 227 0393.
E-mail address: yshimo@med.niigata-u.ac.jp (Y. Shimomura).

http://dx.doi.org/10.1016/j.jdermsci.2015.03.006
0923-1811/

from mutations in either keratin 74 (*KRT74*) or keratin 71 (*KRT71*); each of these genes encodes a type II epithelial keratin and is specifically expressed in the inner root sheath (IRS) of hair follicles (HFs) [4,5]. Similarly, two causative genes for ARWH have been identified: lipase H (*LIPH*) and lysophosphatidic acid receptor 6 (*LPAR6*) [6–9].

LIPH encodes a phosphatidic acid-selective phospholipase A_1 (PA-PLA$_1\alpha$) that is localized at the outer layer of the plasma membrane and produces 2-acyl-lysophosphatidic acid (LPA) from phosphatidic acid [10]. *LPAR6*, previously named *P2RY5*, is a nested gene that is located within intron 17 of retinoblastoma 1 (*RB1*) on chromosome 13q14 [11]. *LPAR6* comprises a single coding exon and encodes a G protein-coupled receptor (GPCR) LPA_6, which is also called P2Y5 and is an LPA receptor [8,12]. Importantly, expression patterns of PA-PLA$_1\alpha$ and LPA_6 overlap in the IRS of HFs, and thus the lipid mediator is believed to play a crucial role in HF development and hair growth in humans [5,7,9]. Furthermore, we (A.I. and J. A.) have reported that *Liph*-knockout mice show a wavy coat phenotype that is similar to WH in humans [13]. Detailed analysis of this mouse model, together with functional studies in cultured cells, demonstrate that PA-PLA$_1\alpha$/LPA/LPA_6 signaling activates tumor necrosis factor-α-converting enzyme (TACE), thereby inducing ectodomain shedding of transforming growth factor-α (TGFα) and causing transactivation of epidermal growth factor receptor (EGFR). Using this phenomenon, an efficient assay system for GPCR-mediated signaling has also been established, while detection of LPA_6 activation was not so much sensitive [13,14].

To date, numerous distinct mutations in both *LIPH* and *LPAR6* have been reported to be causative for ARWH/hypotrichosis in several human populations [6–9,15–37]. In the Japanese population, however, only *LIPH* mutations have been identified in families with the disease, while *LPAR6* mutations have not yet been found in any Japanese patient [19,22,23,25,26]. We herein describe a Japanese family with ARWH/hypotrichosis, the identification of unique compound heterozygous mutations in *LPAR6* in this patient, and the establishment of an assay system to sensitively analyze the function of LPA_6.

2. Materials and methods

2.1. Subjects

The patient was a 36-year old male of Japanese origin (II-3 in Fig. 1A). He has had tightly curled scalp hairs since birth (Fig. 1B). His eyebrows, eyelashes, and beard hairs looked normal. With aging, loss of scalp hairs has progressed and led to an obvious hypotrichosis phenotype (Fig. 1C). When he visited our hospital, he had his scalp hairs shaved (Fig. 1D). Interestingly, several patchy alopecia legions were evident on his scalp skin (Fig. 1D). However, we could not completely exclude the possibility of alopecia areata because we were unable to obtain permission for a skin biopsy. Besides the hair symptoms, he did not show any other associated findings, such as atopic dermatitis, keratosis pilaris, dystrophic nails, palmoplantar keratoderma, or bone anomaly. One of his elder brothers also showed similar hair abnormalities (II-2 in Fig. 1A; data not shown). There were no consanguinities between the parents, who were unaffected and had straight scalp hairs with normal density.

2.2. Mutational analysis of LIPH and LPAR6

After obtaining informed consent, we collected peripheral blood samples or plucked hairs from the family members and 100 population-matched unrelated healthy control individuals (under institutional approval and in adherence to the Declaration of Helsinki Principles). Sampling from one sibling (II-2 in Fig. 1A) was unavailable. Standard techniques were used to isolate genomic DNA from each sample. Genomic DNA samples from the family members were used for direct sequencing analysis of the coding regions of *LIPH* and *LPAR6*; gene-specific primers and polymerase chain reaction (PCR) conditions described previously were used [7,9]. To screen for the mutation c.756T > A (p.Tyr252*) in *LPAR6*, PCR was performed with a forward primer (LPAR6-ORF-F2: 5′-CCAGAAGCCACATGGAAAAC-3′) and a reverse primer (LPAR6-ORF-R2: 5′-CAGCAATACAGAGAGTGATTGG-3′). The amplified products were digested with *Psi*I restriction enzyme at 37 °C for 3 h, and the reaction products were run on 7.0% polyacrylamide gels.

In order to search for other mutations in *LPAR6*, a part of the *LPAR6* promoter sequences was PCR-amplified with the forward primer (LPAR6-P-F1: 5′-TGTGCCATAGAGGTTGTGATATC-3′) and the reverse primer (LPAR6-P-R1: 5′-TGAGTAGCTCTTATCCTGGGTCT-3′); the amplification products were analyzed on 0.8% agarose gels. Subsequently, a PCR product from the patient's DNA was cloned into the pCRII-TOPO vector (Life Technologies, Carlsbad, CA, USA) via TA-cloning, and the positive clones were analyzed by direct sequencing. To screen for the insertion mutation in the *LPAR6* promoter, PCR was performed using an insertion-specific forward primer (LPAR6-ins-F: 5′-GTTTCTTCCTAGTCTCGATGGTC-3′) and an *LPAR6*-specific reverse primer (LPAR6-3UTR-R: 5′-GACACTTTTCA-CAGTTGAAGGAACT-3′); all amplification products were analyzed on 0.8% agarose gels. In addition, a part of intron 23 of the *RB1* gene

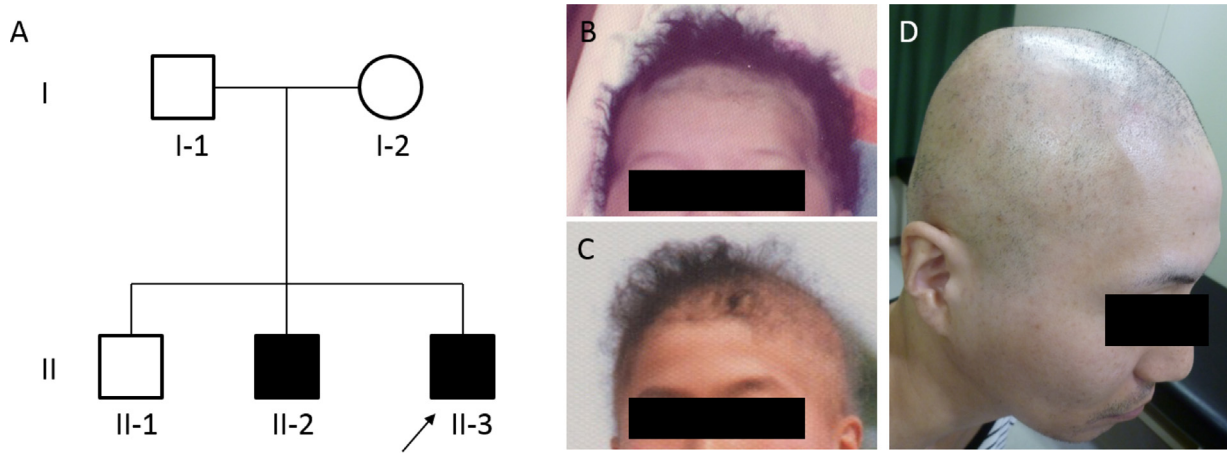

Fig. 1. *Family pedigree and clinical appearance of the patient.* (A) Pedigree of the family. The affected individual analyzed in this study (II-3) is indicated by an arrow. (B–D) Clinical features of the affected individual (II-3) at the age of 1 (B), 13 (C), and 36 (D). Notably, he had obvious woolly scalp hairs when he was a child (B and C).

was PCR-amplified with the forward primer (RB1-F: 5′-GAAAGCCCATCAGACTAACAGC-3′) and the reverse primer (RB1-R: 5′-TCATTTCCCTGATCCACAGCAC-3′). The PCR products were run on 0.7% agarose gels.

2.3. Reverse transcription (RT)-PCR

With plucked hairs collected from the patient and a healthy Japanese control individual, total RNA was isolated using the RNeasy® Minikit (Qiagen Inc., Valencia, CA, USA). To completely remove genomic DNA, RNA samples were each digested with RNase-free DNase I (Takara Bio Inc., Tokyo, Japan) at 37 °C for 1 h; these reactions were followed by reverse transcription using oligo-dT primers and the SuperScript III reverse transcriptase (Life Technologies). The first strand cDNA were used as templates to PCR amplify cDNAs of *LPAR6* and *RB1*. The primer pair for *LPAR6* comprised LPAR6-ORF-F2 and LPAR6-ORF-R2. The *RB1*-cDNA was amplified with the forward primer (RB1-RT-F: 5′-TTGGCGTGCGCTCTTGAGGT-3′) and the reverse primer (RB1-RT-R: 5′-GGTCGCTGTTACATACCATCTG-3′), which were complementary to sequences in *RB1* exons 16 and 25, respectively. The PCR products were run on 1.0% agarose gels, and were also directly sequenced.

2.4. Generation of expression vectors

Expression vectors encoding alkaline phosphatase (AP)-conjugated TGFα and wild-type (WT) or p.Ser154Ala (S154A)-mutant human PA-PLA$_1$α were generated previously [13]. Note that codons within the LPA$_6$-expression construct were optimized (Supplementary Fig. 1) and synthesized by Genscript (Piscataway, NJ, USA) so that the amino acid sequences were unchanged and the efficiency of membrane localization of recombinant LPA$_6$ was maximized. A Flag epitope tag (DYKDDDDK) was inserted between the first and the second codons. An expression construct encoding the p.Tyr252* (Y252X)-mutant LPA$_6$ was generated by introducing a stop codon (TAA) at p.Tyr252 of the codon-optimized WT LPA$_6$ expression construct; the TAT in the codon-optimized template sequence (Supplementary Fig. 1) was mutated to TAA in the p.Tyr252* (Y252X)-mutant LPA$_6$ construct.

2.5. Flow cytometric analysis

HEK293FT (human embryonic kidney) cells were seeded on a 12-well plate (2×10^5 cells per well) one day before transfection. Each expression construct encoding a recombinant LPA$_6$ (WT, 1 to 100 ng per well; Y252X, 100 ng per well) or an empty vector (100 ng per well) were transfected into separate populations of cells with Lipofectamine 2000 (Life Technologies). Approximately 24 h after transfection, cells were blocked with 2% goat serum-containing PBS, labeled with anti-FLAG mAb (clone 2H8, 10 μg/mL; Transgenic Inc., Japan), and then labeled with Alexa 488-conjugated anti-mouse IgG (10 μg/mL; Life Technologies). Fluorescent signal was measured with an SH800 flow cytometer (Sony, Tokyo, Japan).

2.6. TGFα shedding assay

TGFα-shedding assays were performed as described previously [14]. Briefly, HEK293FT cells seeded on a 12-well plate were co-transfected with an AP-TGFα-expression construct and an expression construct encoding LPA$_6$ (WT, 0.1 to 100 ng per well; Y252X-mutant, 100 ng per well) or an empty vector (100 ng per well). Approximately 24 h after transfection, cells were harvested, suspended in 3 mL HBSS, and re-seeded into a 96-well plate (80 μL per well). Cells were then treated with an LPA$_{1-3}$ antagonist Ki16425 (10 μL per well; final concentration of 10 μM) and stimulated with 1-alkyl-OMPT (10 μL per well; final concentration ranging from 100 pM to 1 μM) or LPA (10 μL per well; final concentration ranging from 1 nM to 3.2 μM) for 1 h. The metabolically stable analogue of LPA (1-alkyl-OMPT) potently activates LPA$_6$ [38]. Samples of conditioned media (80 μL per well) were transferred into respective wells of another 96-well plate; for each sample of conditioned media and the cell surfaces in the original wells, *p*-nitrophenylphosphate (*p*-NPP) solution was added to each well, and AP activity was determined by measuring optical absorbance at 405 nm. AP-TGFα release was calculated from a percentage of AP activity in conditioned media followed by subtraction of a baseline (spontaneous) AP-TGFα release response. GraphPad Prism 6 software (GraphPad) was used to fit each concentration–response curves to a respective four-parameter sigmoid mode and determine the associated E_{max} and EC_{50} values.

In another experiment designed to monitor PA-PLA$_1$α-induced LPA$_6$ activation, HEK293FT cells were suspended in Opti-MEM (Life Technologies), seeded in a 96-well plate (80 μL per well), and mixed with a transfection solution (20 μL per well) containing Lipofectamine 2000 and one of the follow combinations of plasmids: (1) AP-TGFα-expression vector (20 ng per well), (2) LPA$_6$-expression vectors (WT, 0.08 to 8 ng per well; Y252X, 8 ng per well) or an empty vector (Mock, 8 ng per well) and (3) PA-PLA$_1$α-expression vectors (WT or catalytically inactive mutant (S154A), 0 to 0.5 ng per well). The cells were cultured for 24 h after the transfection.

Samples of conditioned media (80 μL per well) from the cultured cells were transferred into respective wells of a 96-well plate, and AP activity in the conditioned media and cell surface was quantified by adding *p*-NPP solution and measuring optical absorbance at 405 nm as described previously [13,39].

3. Results

3.1. Identification of a heterozygous nonsense mutation in the LPAR6 gene

Based on clinical features, we diagnosed our patient as having ARWH/hypotrichosis and performed direct sequencing analysis of the *LIPH* and *LPAR6* genes. Although we did not find mutations in the *LIPH* gene, we identified a heterozygous nonsense *LPAR6* mutation c.756T > A (p.Tyr252*) in the patient (Fig. 2A). Screening assay with the *Psi*I restriction enzyme showed that the patient's mother (I-2) was also heterozygous for this mutation, while the other unaffected family members and 100 Japanese control individuals did not carry it (Fig. 2B; data not shown). We did not find any other sequence variants within the coding or 5′- and 3′-noncoding regions (data not shown) of *LPAR6* in the patient.

3.2. Identification of a heterozygous insertion in the LPAR6 promoter region

Because the unaffected mother of the patient carried the c.756T > A mutation in a heterozygous state, we reasoned that the patient's other allele might have a mutation in *LPAR6* promoter region. To test this hypothesis, we designed a series of primers to analyze the *LPAR6* promoter and performed PCR amplification with these primers and genomic DNA templates. To our surprise, PCR with one primer pair (LPAR6-P-F1 and LPAR6-P-R1; Fig. 2C) amplified not only the expected product of 851 bp from the patient's DNA, but also an extraordinarily large product that was approximately 5.0 kb in size (Fig. 2D). We cloned this large product into the pCRII-TOPO vector and analyzed the sequence of a positive clone. The results demonstrated that these *LPAR6* sequences contained a 4156 bp-insertion in the *LPAR6*-promoter region (Fig. 2C). The insertion occurred 248 bp upstream from the *LPAR6*

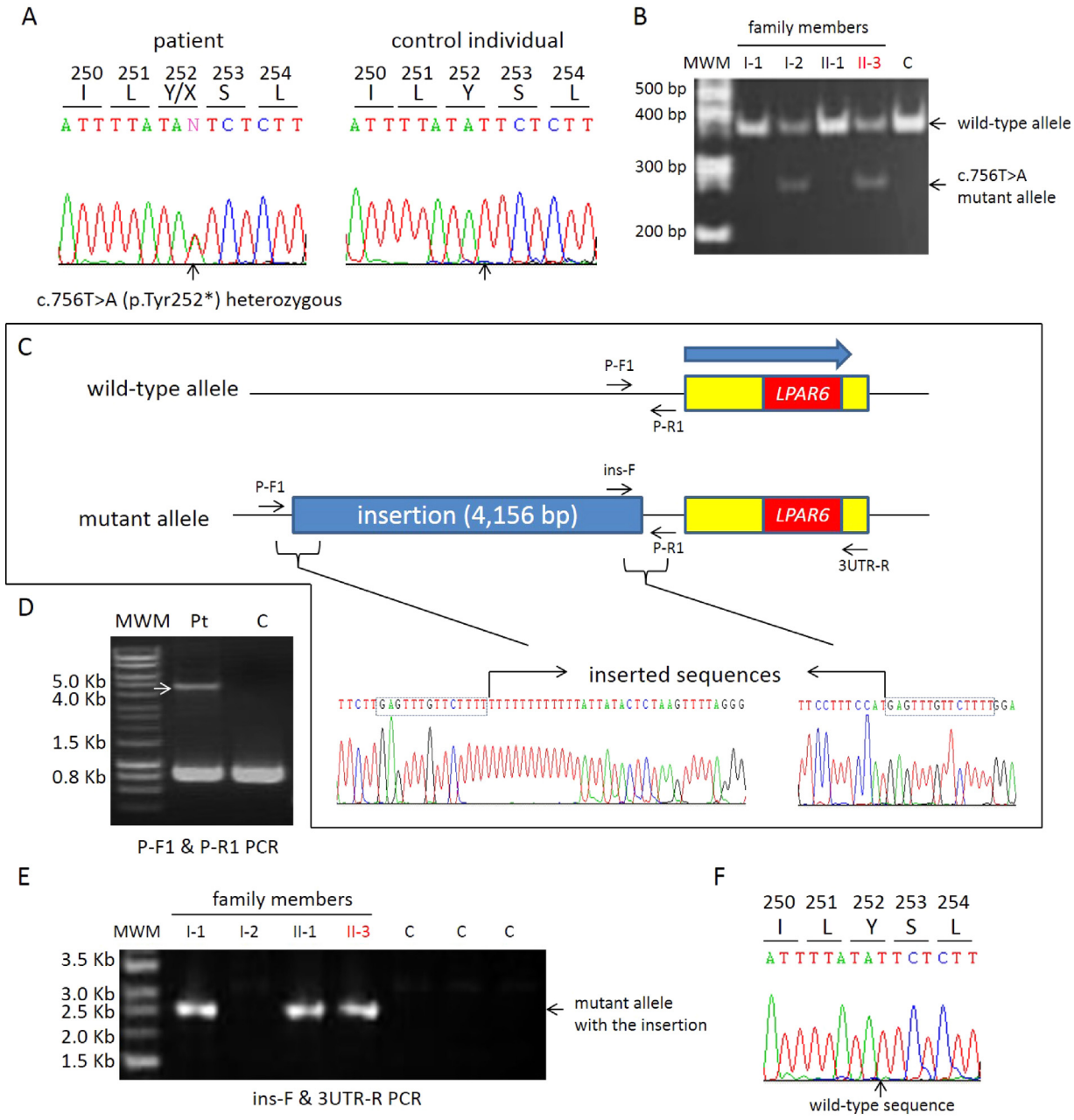

Fig. 2. *Identification of compound heterozygous LPAR6 mutations in the patient.* (A) Identification of a heterozygous nonsense *LPAR6* mutation c.756T > A (p.Tyr252*) in the affected individual. (B) Screening assay with the restriction enzyme *Psi*I revealed that the mutation was inherited from the mother. (C) Schematic representation of wild-type (upper panel) and mutant *LPAR6* allele with the insertion (lower panel). Positions of primers used in the analysis are indicated by black arrows. Direction of *LPAR6* gene transcription is indicated by a filled arrow. The non-coding and coding sequences of *LPAR6* are indicated with yellow and red boxes, respectively. The inserted sequences (4156 bp) are indicated by a blue box. Each boundary sequence of the insertion is bracketed underneath the blue box and expanded below. The duplicated sequences, 14 bp in size, are indicated by dotted boxes. (D) Results of PCR amplification with primers, P-F1 and P-R1 (C). Note that a large fragment (shown by a white arrow) was amplified only from the patient's genomic DNA (Pt). (E) PCR using primers, ins-F and 3UTR-R (C), specifically amplified a fragment derived from the mutant allele with the insertion. This assay revealed that the patient's father (I-1) and brother (II-1) also carried the mutation. (F) Direct sequencing of the PCR product from the patient (E) showed wild-type sequence at position c.756 of the *LPAR6* gene. MWM, molecular weight markers (B, D and E); C, control individuals (B, D and E). The patient (II-3) is indicated by red text (B and E).

transcription start site, and there was a 14 bp-duplication of *LPAR6* promoter sequences at both borders of the insertion (Fig. 2C). We then performed screening assay using an insertion-specific forward primer (LPAR6-ins-F) and an *LPAR6*-specific reverse primer (LPAR6-3UTR-R) and found that both his unaffected father (I-1) and brother (II-1) also had this insertion (Fig. 2E). Neither his mother (I-2) nor 100 control individuals carried this insertion (Fig. 2E; data not shown). Direct-sequencing analysis of the PCR product from the patient showed WT sequence at position c.756 in the *LPAR6* gene (Fig. 2F). Detailed analysis of the insertion using NCBI-BLAST (http://blast.ncbi.nlm.nih.gov/Blast.cgi) revealed that the sequences were derived from intron 23 of the *RB1* gene (Supplementary Fig. 2A). In order to determine whether the corresponding sequences were deleted from intron

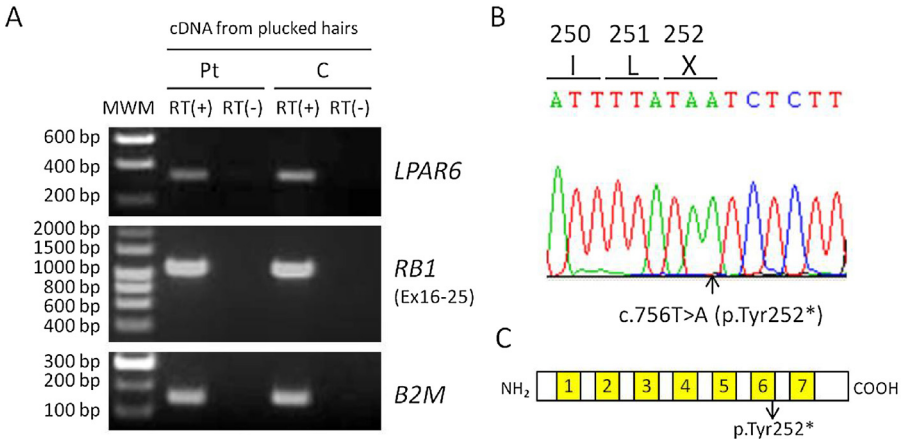

Fig. 3. Only *LPAR6*-mRNA from the c.756T > A (p.Tyr252*) mutant allele was expressed in the patient's hair follicles. (A) Reverse transcription (RT)-PCR amplification of cDNAs derived from *LPAR6* (top panel), *RB1* (middle panel), and *B2M* (bottom panel) from the follicular RNA of the patient or a control individual. The *B2M*-cDNA was amplified as a control. PCR without RT did not lead to any products, indicating that there was no genomic DNA contamination in the samples. +/− denotes reactions with or without RT. MWM, molecular weight markers; Pt, patient; C, control individual. (B) Direct sequencing of the *LPAR6* cDNA amplified from the patient's sample revealed only the c.756T > A (p.Tyr252*)-mutant *LPAR6*. (C) Schematic representation of the LPA_6 protein. Transmembrane domains are indicated by yellow boxes. Position of the mutation p.Tyr252* is indicated by an arrow. (For interpretation of the references to color in this figure legend, the reader is referred to the web version of this article.)

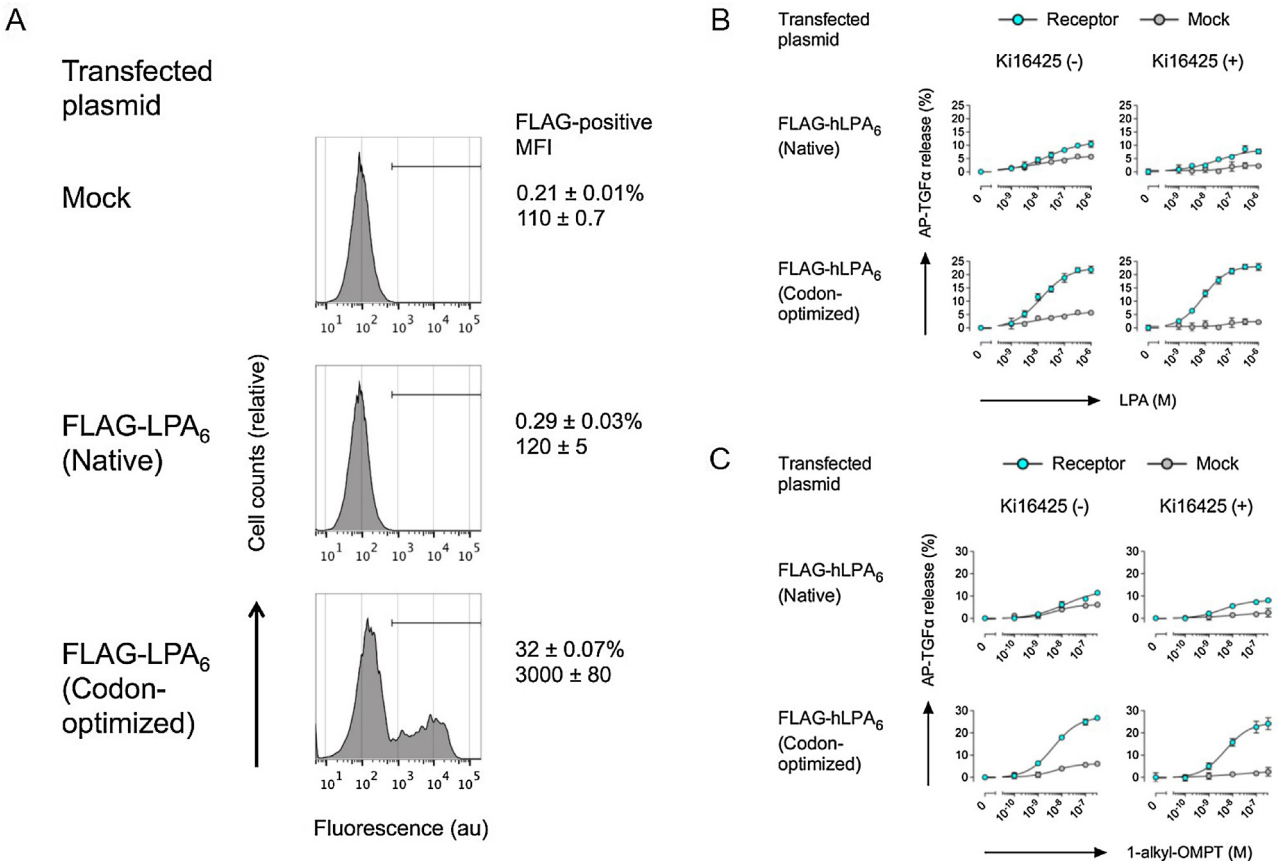

Fig. 4. *Improved expression and detection of LPA_6 by using codon optimization and Ki16425 treatment.* (A) Cells transfected with the indicated N-terminally FLAG epitope-tagged LPA_6 (native or codon-optimized sequence) or an empty vector (mock) were subject to flow cytometric analysis with an anti-FLAG antibody. FLAG-positive cells and mean fluorescent intensity are shown on the right (mean ± SD values of three culture replicates in a single assay). Data are representative of two independent experiments with similar results. (B, C) Cells transfected with AP-TGFα-encoding plasmid vector together with N-terminally FLAG epitope-tagged LPA_6 (native or codon-optimized sequence) or an empty vector (mock) were harvested and seeded in a 96-well plates; the seeded cells were treated with the indicated concentration of LPA (B) or 1-alkyl-OMPT (C) for 1 h in the presence (±) or absence (−) of 10 μM Ki16425, a LPA_{1-3} inhibitor. Release of AP-TGFα into the conditioned media was quantified by separating conditioned media from cells and measuring AP activity in both conditioned media and cells using *p*-nitrophenylphosphate as a substrate. Spontaneous AP-TGFα release in a vehicle-treated condition was set at a baseline. Note that Ki16425 treatment supressed LPA- and 1-alkyl-OMPT-induced responses in mock-transfected cells and that codon opmization enhanced LPA_6 responses. Symbols and error bars indicate mean and SD values, respectively, of three culture replicates in a single assay. Data are representative of two independent experiments with similar results.

23 of *RB1*, we amplified this region by PCR and found that intron 23 was present in both *RB1* alleles from the patient (Supplementary Fig. 2B).

3.3. Evidence for loss of transcription from the mutant LPAR6 allele with the insertion

To investigate how each mutation affected *LPAR6* expression, we used total RNA samples from hairs plucked from the patient or a control individual to perform RT-PCR analysis. *LPAR6* cDNA was amplified from each sample (Fig. 3A). However, direct sequencing of patient *LPAR6* cDNA indicated that only *LPAR6* cDNA from the c.756T > A (p.Tyr252*) was present; this finding indicated that the paternal mutant allele with the insertion in the *LPAR6* promoter was not transcribed (Fig. 3B). In PCR for the *RB1* cDNA, a clear single fragment was amplified from patient-derived or control-derived cDNA samples with similar efficiency. These findings indicated that the *LPAR6* promoter insertion did not affect splicing of *RB1* transcripts (Fig. 3A). Taken together, these results strongly indicated that only the p.Tyr252*-mutant LPA_6 protein would be stably expressed in the patient's HFs.

3.4. Establishment of a sensitive assay system for LPA_6

The c.756T > A (p.Tyr252*) mutation is located within the 6th transmembrane domain of the LPA_6 protein (Fig. 3C). To investigate how the mutation affected the function, we tried to perform a series of in vitro analysis in cultured cells. We initially transfected an N-terminally FLAG-tagged WT LPA_6 with native nucleotide sequences into HEK293FT cells and performed flow cytometry with an anti-FLAG antibody. However, to our surprise, the plasma membrane localization of the native LPA_6 was undetectable (Fig. 4A). Furthermore, the native LPA_6 poorly responded to LPA and 1-alkyl-OMPT (Fig. 4B and C). Through a serial of improvement trials, we found a codon-optimized LPA_6, which kept the amino acid sequences identical (Supplementary Fig. 1), efficiently localized to the plasma membranes (Fig. 4A) and the response to its agonists was also significantly enhanced (Fig. 4B and C). In addition, we found that pretreatment with an LPA_{1-3} antagonist Ki16425 almost completely suppressed the background response and improved the detection specificity of LPA_6-dependant activation (Fig. 4B and C). Collectively, we have established a sensitive assay system for LPA_6 and used it throughout this study.

3.5. The p.Tyr252*-mutant LPA_6 failed to localize to plasma membranes and did not function as an LPA receptor

We transiently overexpressed either WT or p.Tyr252* (Y252X)-mutant LPA_6 proteins and analyzed their plasma membrane localization. Cells that expressed WT LPA_6 on cell surfaces were detected even when the amount of transfected expression construct was as low as 1 ng per well; the cell surface expression of WT LPA_6 became more evident in a dose-dependent manner (Fig. 5). In contrast, expression of the Y252X-mutant LPA_6 on cell surfaces was not evident in any sample, even when 100 ng per well of expression construct was used for transfection (Fig. 5). The results clearly showed that the Y252X-mutant LPA_6 did not localize to plasma membranes.

We then investigated whether the p.Tyr252* (Y252X)-mutant LPA_6 responded to LPA_6 agonists. Both LPA and 1-alkyl-OMPT significantly activated the WT-LPA_6 (Fig. 6). Notably, WT LPA_6 responded to 1-alkyl-OMPT even when 0.1 ng of the expression construct was transfected per well (Fig. 6). However, the Y252X-mutant LPA_6 did not show any response to either molecule; these findings indicated that the mutant protein did not function as an LPA receptor (Fig. 6).

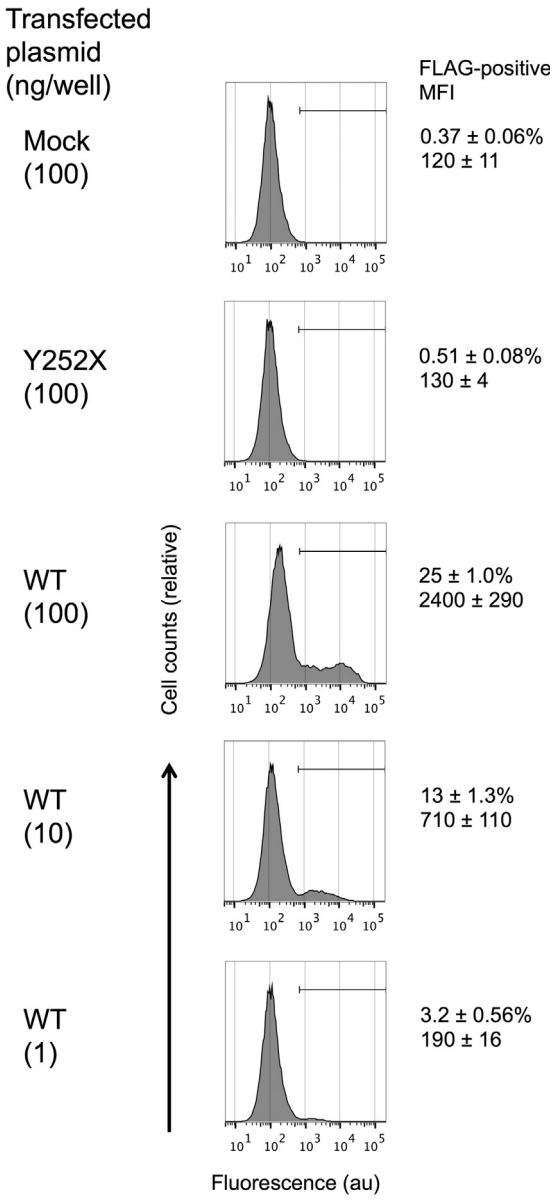

Fig. 5. *The p.Tyr252*-mutant LPA_6 protein failed to localize at plasma membranes.* Cells transfected with the indicated amount of N-terminally FLAG epitope-tagged LPA_6 (wild-type (WT) or p.Tyr252* (Y252X)-mutant) or an empty vector (Mock) were subject to flow cytometric analysis with an anti-FLAG antibody. FLAG-positive cells and mean fluorescent intensity are shown on the right (mean ± SD values of three culture replicates in a single assay). Data are representative of two independent experiments with similar results.

3.6. The p.Tyr252*-mutant LPA_6 disrupted the PA-$PLA_1\alpha$/LPA/LPA_6 axis

Finally, we used PA-$PLA_1\alpha$ to test whether the p.Tyr252* (Y252X)-mutant LPA_6 reacted to naturally occurring LPA species. As shown in previous studies [22,23,39], co-transfection of WT PA-$PLA_1\alpha$ and WT LPA_6 expression constructs markedly activated LPA_6 signaling; however, this level of activation was not evident when WT LPA_6 was co-expressed with a S154A-mutant PA-$PLA_1\alpha$; this recombinant mutant protein carried a critical amino acid substitution at a catalytic residue of PA-$PLA_1\alpha$ protein (Fig. 7). By contrast, the Y252X-mutant LPA_6 did not show any activity even when co-expressed with WT PA-$PLA_1\alpha$ (Fig. 7). Taken together, these findings indicated that Y252X-mutant LPA_6 failed to respond to endogenously produced LPA species.

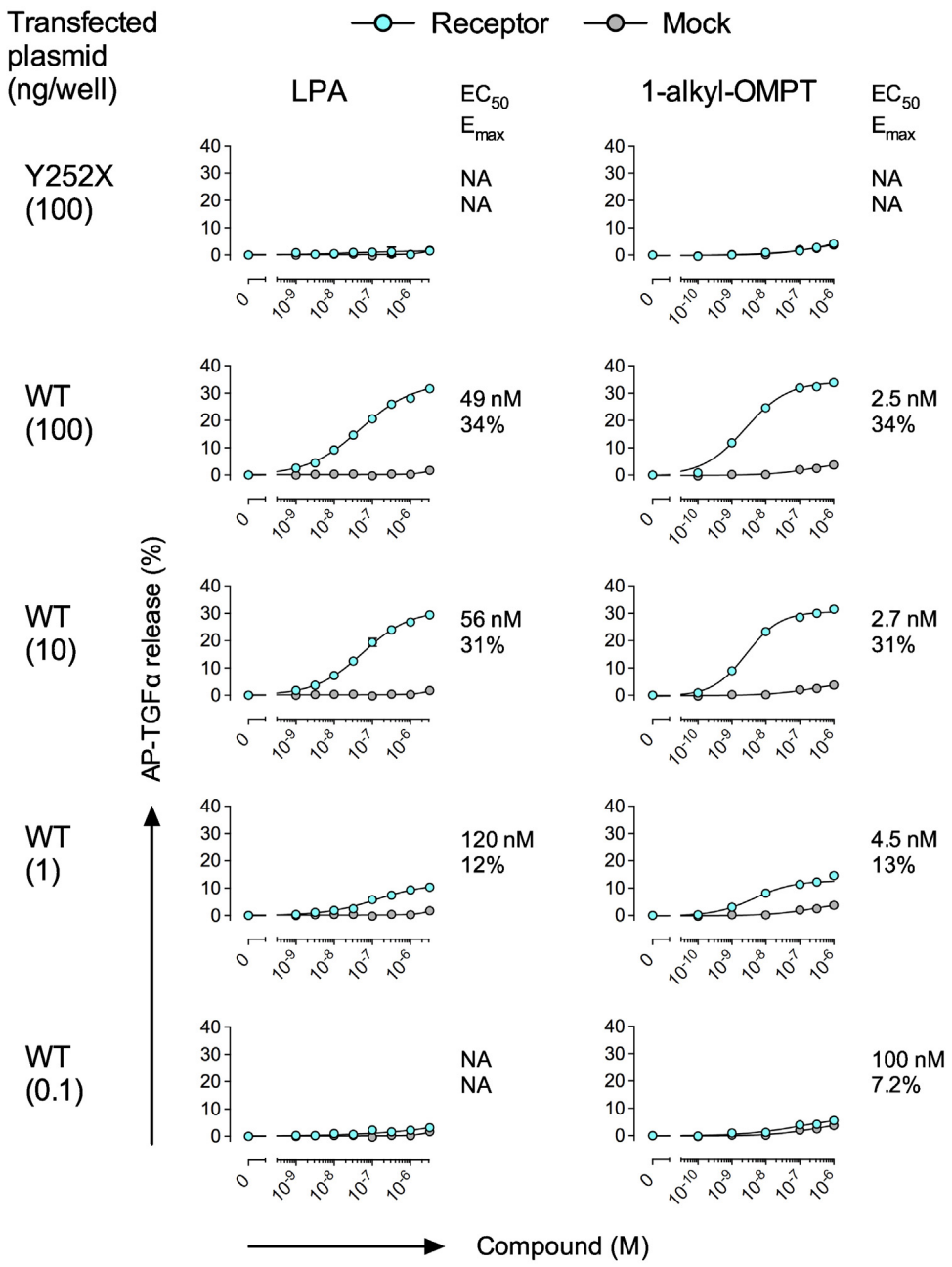

Fig. 6. *The p.Tyr252*-mutant LPA_6 protein did not respond to LPA_6 agonists.* Cells transfected with AP-TGFα-encoding plasmid vector together with indicated amount of LPA_6-encoding plasmid vector (wild-type (WT) or p.Tyr252* (Y252X)-mutant) or an empty plasmid vector (Mock) were harvested and seeded in a 96-well plates; the seeded cells were treated with the indicated concentration of 1-alkyl-OMPT or LPA for 1 h in the presence of 10 μM Ki16425. AP-TGFα release was determined as indicated in Fig. 4 legend and the method section. EC_{50} and E_{max} values were obtained by fitting data to a four-parameter logistic curve. Symbols and error bars indicate mean and SD values, respectively, of three culture replicates in a single assay. Data are representative of two independent experiments with similar results. Note that error bars are smaller than symbols in most data points. NA, not available.

4. Discussion

In this study, we analyzed a Japanese family with ARWH/hypotrichosis and identified compound heterozygous *LPAR6* mutations in the patient (Figs. 1 and 2). We initially searched for mutations in the *LIPH* gene because previously only *LIPH* mutations have been identified in Japanese patients with this disease [19,22,23,25,26]. Moreover, the clinical features of the affected individual analyzed in this study were indistinguishable from those of patients with *LIPH* mutations. To the best of our knowledge, we herein report the first Japanese case of ARWH/hypotrichosis caused by *LPAR6* mutations, and our results further indicated a close relationship in function between the *LIPH* and *LPAR6*.

Of the two *LPAR6* mutations identified in this patient, one was a large insertion mutation within the *LPAR6* promoter region; this allele was paternally inherited (Fig. 2C–F). The insertion destroyed the structure of the promoter and resulted in loss of *LPAR6* transcription from the mutant allele, as demonstrated by RT-PCR experiments (Fig. 3A and B). Interestingly, the inserted sequences were derived from intron 23 of the *RB1* gene (Supplementary Fig. 2A). Our results indicated that a part of the sequences of intron 23 of the *RB1* gene had accidentally been duplicated and inserted into the *LPAR6* promoter, which is located in intron 17 of *RB1*

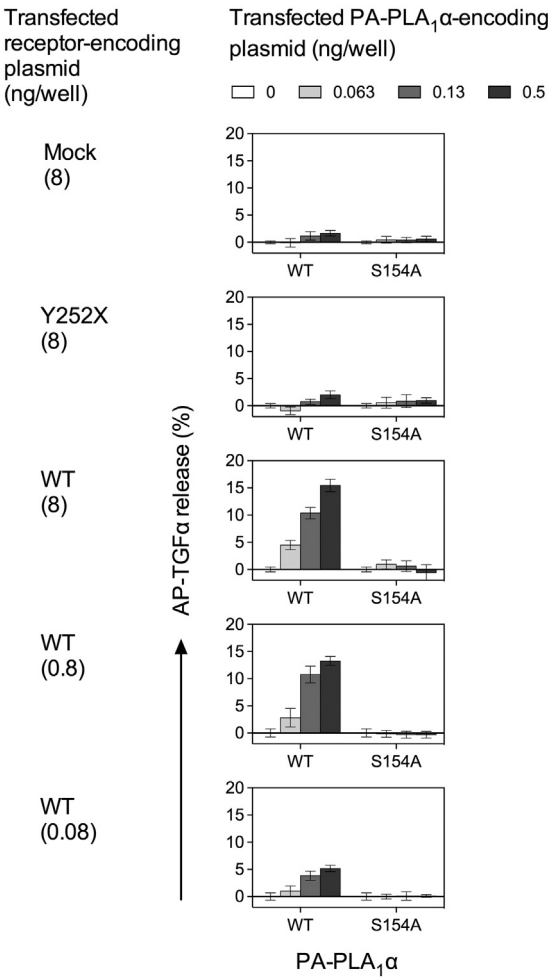

Fig. 7. *Disruption of the PA-PLA$_1$α/LPA/LPA$_6$ axis by the p.Tyr252*-mutant LPA$_6$ protein.* Cells were seeded in 96-well plates and transfected with various combinations of AP-TGFα-encoding plasmid vector, LPA$_6$-encoding plasmid vector (wild-type (WT), p.Tyr252* (Y252X)-mutant), or an empty vector (Mock) and PA-PLA$_1$α-encoding plasmid vector (WT or p.Ser154Ala (S154)-mutant). After 24 h incubation, release of AP-TGFα was quantified by separating conditioned media from cells and measuring AP activity in both conditioned media and cells using *p*-nitrophenylphosphate. Spontaneous AP-TGFα release in an enzyme plasmid-free condition was set at a baseline. Symbols and error bars indicate mean and SD values, respectively, of six culture replicates in a single assay. Data are representative of two independent experiments with similar results.

(Supplementary Fig. 2A). Such copy number variation is relatively rare, and this is the first *LPAR6* mutation detected in the *LPAR6* promoter region.

The c.756T > A (pTyr252*) nonsense mutation identified in the maternal *LPAR6* allele is predicted to generate a truncated LPA$_6$ protein that lacks the C-terminus, including the 7th transmembrane domain (Figs. 2A and B and 3C). Based on the results of RT-PCR experiment, only the p.Tyr252*-mutant LPA$_6$ was expected to be expressed stably in the patient's HFs. Previously, 24 distinct disease-causing mutations have been identified in the *LPAR6* gene [8,9,27–37]. However, expression and functional analyses for these mutations have rarely been performed. Additionally, two premature termination codon mutations, p.Gln155* and p.Lys125Asnfs*37, reportedly cause aberrant LPA$_6$ localization within the cytoplasm [8]. Moreover, LPA reportedly does not activate the p.Lys125Asnfs*37-mutant LPA$_6$ [8]. Similarly, the p.Tyr252*-mutant LPA$_6$ did not localize at plasma membranes (Fig. 5) and did not respond to any of the defined LPA$_6$ agonists tested (Fig. 6). Finally, we clearly demonstrated that the p.Tyr252*-mutant LPA$_6$ disrupted the PA-PLA$_1$α/LPA/LPA$_6$ axis, which caused ARWH/hypotrichosis in our patient (Fig. 7). We would like to emphasize that the activation of WT LPA$_6$ (Figs. 4, 6 and 7) was detected much more sensitively than that shown in previous studies [8,13,14,22,23,39]. In this study, we have added two critical modifications into the *in vitro* assay system that we (A.I. and J.A.) have recently reported [13,14]: (1) we used codon-optimized LPA$_6$ to significantly increase the efficiency of plasma membrane localization of recombinant LPA$_6$ (Fig. 4A, Supplementary Fig. 1); (2) we treated the cells with an LPA$_{1-3}$ antagonist Ki16425 to inhibit the effect of endogenous LPA receptors expressed in HEK293FT cells [13] (Fig. 4B and C). As a result, we have finally established an assay system to sensitively detect LPA$_6$ activation (Fig. 4). We believe that our assay system will become a useful tool to search for ideal agonists of LPA$_6$ which can be used to produce a medicine for the treatment of ARWH/hypotrichosis in the future.

Our results provide important information regarding the molecular basis for ARWH/hypotrichosis in the Japanese population; they also further highlight the crucial roles of the PA-PLA$_1$α/LPA/LPA$_6$ signaling in HF development and hair growth in humans.

Acknowledgements

We are grateful to Miho Morikawa for technical assistance with the TGFα shedding assay. This study was supported in part by a grant from Takeda Science Foundation, Japan (to Y.S.) and by "Research on Measures for Intractable Diseases" Project: matching fund subsidy (H26-077) from Ministry of Health, Labour, and Welfare, Japan. A.I. was funded by PRESTO (Precursory Research for Embryonic Science and Technology) from Japan Science and Technology Agency (JST) and a Grant-in-Aid for Scientific Research (C) (KAKENHI 26440043). J.A. was funded by CREST from JST and a Grant-in-Aid for Scientific Research on Innovative Areas from the Ministry of Education, Science, Sports and Culture of Japan (MEXT).

Appendix A. Supplementary data

Supplementary data associated with this article can be found, in the online version, at http://dx.doi.org/10.1016/j.jdermsci.2015.03.006.

References

[1] Shimomura Y. Congenital hair loss disorders: rare, but not too rare. J Dermatol 2012;39:3–10.
[2] Shimomura Y, Christiano AM. Biology and genetics of hair. Annu Rev Genomics Hum Genet 2010;11:109–32.
[3] Shimomura Y, Wajid M, Zlotogorski A, Lee YJ, Rice RH, Christiano AM. Founder mutations in the lipase H (LIPH) gene in families with autosomal recessive woolly hair/hypotrichosis. J Invest Dermatol 2009;129:1927–34.
[4] Shimomura Y, Wajid M, Petukhova L, Kurban M, Christiano AM. Autosomal dominant woolly hair resulting from disruption of keratin 74 (KRT74), a novel determinant of human hair texture. Am J Hum Genet 2010;86:632–8.
[5] Fujimoto A, Farooq M, Fujikawa H, Inoue A, Ohyama M, Ehama R, et al. A missense mutation within the helix initiation motif of the keratin K71 gene underlies autosomal dominant woolly hair/hypotrichosis. J Invest Dermatol 2012;132:2342–9.
[6] Kazantseva A, Goltsov A, Zinchenko R, Grigorenko AP, Abrukova AV, Moliaka YK, et al. Human hair growth deficiency is linked to a genetic defect in the phospholipase gene LIPH. Science 2006;314:982–5.
[7] Shimomura Y, Wajid M, Petukhova L, Shapiro L, Christiano AM. Mutations in the lipase H gene underlie autosomal recessive woolly hair/hypotrichosis. J Invest Dermatol 2009;129:622–8.
[8] Pasternack SM, von Kügelgen I, Al Aboud K, Lee YA, Rüschendorf F, Voss K, et al. G protein-coupled receptor P2Y5 and its ligand LPA are involved in maintenance of human hair growth. Nat Genet 2008;40:329–34.
[9] Shimomura Y, Wajid M, Ishii Y, Shapiro L, Petukhova L, Gordon D, et al. Disruption of P2RY5, an orphan G protein-coupled receptor, underlies autosomal recessive woolly hair. Nat Genet 2008;40:335–9.
[10] Sonoda H, Aoki J, Hiramatsu T, Ishida M, Bandoh K, Nagai Y, et al. A novel phosphatidic acid-selective phospholipase A1 that produces lysophosphatidic acid. J Biol Chem 2002;277:34254–63.

[11] Herzog H, Darby K, Hort YJ, Shine J. Intron 17 of the human retinoblastoma susceptibility gene encodes an actively transcribed G protein-coupled receptor gene. Genome Res 1996;6:858–61.
[12] Yanagida K, Masago K, Nakanishi H, Kihara Y, Hamano F, Tajima Y, et al. Identification and characterization of a novel lysophosphatidic acid receptor, p2y5/LPA6. J Biol Chem 2009;284:17731–41.
[13] Inoue A, Arima N, Ishiguro J, Prestwich GD, Arai H, Aoki J. LPA-producing enzyme PA-PLA$_1\alpha$ regulates hair follicle development by modulating EGFR signaling. EMBO J 2011;30:4248–60.
[14] Inoue A, Ishiguro J, Kitamura H, Arima N, Okutani M, Shuto A, et al. TGFα shedding assay: an accurate and versatile method for detecting GPCR activation. Nat Methods 2012;9:1021–9.
[15] Ali G, Chishti MS, Raza SI, John P, Ahmad W. A mutation in the lipase H (LIPH) gene underlie autosomal recessive hypotrichosis. Hum Genet 2007;121:319–25.
[16] Nahum S, Pasternack SM, Pforr J, Indelman M, Wollnik B, Bergman R, et al. A large duplication in LIPH underlies autosomal recessive hypotrichosis simplex in four Middle Eastern families. Arch Dermatol Res 2009;301:391–3.
[17] Pasternack SM, von Kügelgen I, Müller M, Oji V, Traupe H, Sprecher E, et al. In vitro analysis of LIPH mutations causing hypotrichosis simplex: evidence confirming the role of lipase H and lysophosphatidic acid in hair growth. J Invest Dermatol 2009;129:2772–6.
[18] Naz G, Khan B, Ali G, Azeem Z, Wali A, Ansar M, et al. Novel missense mutations in lipase H (LIPH) gene causing autosomal recessive hypotrichosis (LAH2). J Dermatol Sci 2009;54:12–6.
[19] Shimomura Y, Ito M, Christiano AM. Mutations in the LIPH gene in three Japanese families with autosomal recessive woolly hair/hypotrichosis. J Dermatol Sci 2009;56:205–7.
[20] Kalsoom UE, Habib R, Khan B, Ali G, Ali N, Ansar M, et al. Mutations in lipase H gene underlie autosomal recessive hypotrichosis in five Pakistani families. Acta Derm Venereol 2010;90:93–4.
[21] Tariq M, Azhar A, Baig SM, Dahl N, Klar J. A novel mutation in the lipase H gene underlies autosomal recessive hypotrichosis and woolly hair. Sci Rep 2012;2:730.
[22] Shinkuma S, Inoue A, Aoki J, Nishie W, Natsuga K, Ujiie H, et al. The β9 loop domain of PA-PLA1α has a crucial role in autosomal recessive woolly hair/hypotrichosis. J Invest Dermatol 2012;132:2093–5.
[23] Yoshizawa M, Nakamura M, Farooq M, Inoue A, Aoki J, Shimomura Y. A novel mutation, c.699C > G (p.C233W), in the LIPH gene leads to a loss of the hydrolytic activity and the LPA6 activation ability of PA-PLA1α in autosomal recessive wooly hair/hypotrichosis. J Dermatol Sci 2013;72:61–4.
[24] Mehmood S, Jan A, Muhammad D. Mutations in the lipase-H gene causing autosomal recessive hypotrichosis and woolly hair. Australas J Dermatol 2014 (in press).
[25] Hayashi R, Inui S, Farooq M, Ito M, Shimomura Y. Expression studies of a novel splice site mutation in the LIPH gene identified in a Japanese patient with autosomal recessive woolly hair. J Dermatol 2014;41:890–4.
[26] Hayashi R, Akasaka T, Ito M, Shimomura Y. Compound heterozygous mutations in two distinct catalytic residues of the LIPH gene underlie autosomal recessive woolly hair in a Japanese family. J Dermatol 2014;41:937–8.
[27] Azeem Z, Jelani M, Naz G, Tariq M, Wasif N, Kamran-Ul-Hassan Naqvi S, et al. Novel mutations in G protein-coupled receptor gene (P2RY5) in families with autosomal recessive hypotrichosis (LAH3). Hum Genet 2008;123:515–9.
[28] Petukhova L, Sousa Jr EC, Martinez-Mir A, Vitebsky A, Dos Santos LG, Shapiro L, et al. Genome-wide linkage analysis of an autosomal recessive hypotrichosis identifies a novel P2RY5 mutation. Genomics 2008;92:273–8.
[29] Tariq M, Ayub M, Jelani M, Basit S, Naz G, Wasif N, et al. Mutations in the P2RY5 gene underlie autosomal recessive hypotrichosis in 13 Pakistani families. Br J Dermatol 2009;160:1006–10.
[30] Pasternack SM, Murugusundram S, Eigelshoven S, Müller M, Kruse R, Lehmann P, et al. Novel mutations in the P2RY5 gene in one Turkish and two Indian patients presenting with hypotrichosis and woolly hair. Arch Dermatol Res 2009;301:621–4.
[31] Horev L, Saad-Edin B, Ingber A, Zlotogorski A. A novel deletion mutation in P2RY5/LPA(6) gene cause autosomal recessive woolly hair with hypotrichosis. J Eur Acad Dermatol Venereol 2010;24:858–9.
[32] Kurban M, Ghosn S, Abbas O, Shimomura Y, Christiano A. A missense mutation in the P2RY5 gene leading to autosomal recessive woolly hair in a Syrian patient. J Dermatol Sci 2010;57:132–4.
[33] Nahum S, Morice-Picard F, Taieb A, Sprecher E. A novel mutation in LPAR6 causes autosomal recessive hypotrichosis of the scalp. Clin Exp Dermatol 2011;36:188–94.
[34] Mahmoudi H, Tug E, Parlak AH, Atasoy HI, Ludwig M, Polat M, et al. Identification of an Alu-mediated 12.2-kb deletion of the complete LPAR6 (P2RY5) gene in a Turkish family with hypotrichosis and woolly hair. Exp Dermatol 2012;21:469–71.
[35] Azhar A, Tariq M, Baig SM, Dahl N, Klar J. A novel mutation in lysophosphatidic acid receptor 6 gene in autosomal recessive hypotrichosis and evidence for a founder effect. Eur J Dermatol 2012;22:464–6.
[36] Kurban M, Wajid M, Shimomura Y, Christiano AM. Mutations in LPAR6/P2RY5 and LIPH are associated with woolly hair and/or hypotrichosis. J Eur Acad Dermatol Venereol 2013;27:545–9.
[37] Liu LH, Chen G, Wang JW, Liu SX, Wang JB, Zhou FS, et al. A novel deletion mutation in the LPAR6 gene underlies autosomal recessive woolly hair with hypotrichosis. Clin Exp Dermatol 2013;38:796–8.
[38] Jiang G, Inoue A, Aoki J, Prestwich GD. Phosphorothioate analogs of sn-2 radyl lysophosphatidic acid (LPA): metabolically stabilized LPA receptor agonists. Bioorg Med Chem Lett 2013;23:1865–9.
[39] Shinkuma S, Akiyama M, Inoue A, Aoki J, Natsuga K, Nomura T, et al. Prevalent LIPH founder mutations lead to loss of P2Y5 activation ability of PA-PLA1alpha in autosomal recessive hypotrichosis. Hum Mutat 2010;31:602–10.